# A spatially calibrated model of annual accumulation rate on the Greenland Ice Sheet (1958–2007)

Evan W. Burgess,[1] Richard R. Forster,[1] Jason E. Box,[2,3] Ellen Mosley-Thompson,[2,3] David H. Bromwich,[2,3] Roger C. Bales,[4] and Laurence C. Smith[5]

[1]   Past estimates of Greenland Ice Sheet accumulation rates have been multiyear climatologies based on ice/firn cores and coastal precipitation records. Existing annually resolved estimates have incompletely quantified uncertainty, owing primarily to incomplete spatial coverage. This study improves upon these shortcomings by calibrating annual (1958–2007) solid precipitation output from the Fifth Generation Mesoscale Model modified for polar climates (Polar MM5) using firn core and meteorological station data. The calibration employs spatial interpolation of regionally derived linear correction functions. Residual uncertainties exhibit coherent spatial patterns, which are modeled via spatial interpolation of root mean squared errors. Mean 1958–2007 Greenland Ice Sheet annual accumulation rate is 337 ± 48 mm/yr water equivalent (w.e.) or 591 ± 83 Gt/yr. Annual estimates contain one standard deviation uncertainties of 74 mm/yr w.e., 22%, or 129 Gt/yr. Accumulation rates in southeast Greenland are found to exceed 2000 mm/yr w.e. and to dominate interannual variability in Greenland Ice Sheet total accumulated mass, representing 31% of the whole. Accumulation rates in the southeast are of sufficient magnitude to affect the sign of Greenland mass balance during some years. The only statistically significant temporal change in total ice sheet accumulation in the 1958–2007 period occurred between 1960 and 1972, when a simultaneous accumulation increase and decrease occurred in west and east Greenland, respectively. No statistically significant uniform change in ice sheet-wide accumulation is evident after 1972. However, regional changes do occur, including an accumulation increase on the west coast post-1992. The high accumulation rates of 2002–2003 appear to be confined to the southeast.

## 1.  Introduction

[2]  The matter of estimating accumulation on the Greenland Ice Sheet is complex and requires a brief introduction. When used in the context of Greenland, "accumulation" refers to all positive components of Greenland's mass balance, which includes primarily solid precipitation, but also drifted snow (transported from elsewhere), retained rainwater, and riming (the deposition of water vapor onto the snow). As such, "accumulation, " as defined here, is not constrained to the accumulation zone; it includes any gain of mass regardless of whether it is subsequently lost owing to ablation processes during the same hydrologic year. To make matters more complex, it is traditional to deduct mass lost from sublimation and wind scouring from accumulation to reach a term referred to in the literature as "net accumulation. " Thus, despite the fact that sublimation and wind scouring are processes of mass loss, they are considered separate from processes of ablation. The reasoning behind this confusion is in situ measurements of mass gain collected from firn/ice cores measure net accumulation. Finally, since the process of accumulation occurs through time, it is common to add the term "rate" defining the amount of mass accrued over one year. Herein, this paper will discuss only net accumulation rate; however, for brevity we will simplify this term to "accumulation rate."

[3]  Greenland Ice Sheet accumulation rates have been investigated extensively. Initial accumulation rate maps involved spatial interpolation of data from firn cores, snow pits, and coastal meteorological stations [*Benson*, 1962; *Ohmura and Reeh*, 1991; *Ohmura et al.*, 1999].

---

[1]Department of Geography, University of Utah, Salt Lake City, Utah, USA.

[2]Department of Geography, Ohio State University, Columbus, Ohio, USA.

[3]Byrd Polar Research Center, Ohio State University, Columbus, Ohio, USA.

[4]Sierra Nevada Research Institute, University of California, Merced, California, USA.

[5]Department of Geography, University of California, Los Angeles, California, USA.

More advanced interpolation studies followed [*Calanca et al.*, 2000; *Cogley*, 2004; *van der Veen et al.*, 2001], including incorporation of updated in situ observations [*Ohmura et al.*, 1999; *Bales et al.*, 2001a, 2009]. *McConnell et al.* [2001] mapped annually resolved accumulation rates for the southern part of the ice sheet by kriging annually resolved firn core data.

[4] Global climate models have also been used to estimate spatial patterns in Greenland Ice Sheet accumulation rates [*Ohmura et al.*, 1996; *Thompson and Pollard*, 1997; *Glover*, 1999; *Murphy et al.*, 2002]. Regional climate models provide higher spatial resolution accumulation rate grids [*Dethloff et al.*, 2002; *Box et al.*, 2004, 2005, 2006; *Box*, 2005; *Fettweis et al.*, 2008; *Ettema et al.*, 2009]. Application of climate reanalysis data has also produced accumulation grids and whole ice sheet mass budget estimates [*Hanna et al.*, 2005, 2006, 2008]. Atmospheric simulations are advantageous because they provide continuous spatial coverage and fine temporal resolution, yet they lack direct connection to in situ data, a problem partially addressed by models using reanalysis data. In situ observations from snow pits or firn/ice cores provide an excellent opportunity to validate models [*Box and Rinke*, 2003; *Box et al.*, 2004, 2006; *Hanna et al.*, 2006]. *Box et al.* [2006] calibrated ice sheet accumulation rate biases in a regional climate data assimilation and downscaling model (Fifth Generation Mesoscale Model modified for polar climates, Polar MM5) by applying a linear correction function to compensate bias evident from comparison with 34 single-year snow pit observations, but more complex regional systematic biases remained uncorrected.

[5] This paper evaluates spatial patterns of Polar MM5 solid precipitation biases evident through model comparison with firn/ice cores (herein generalized as firn cores) and coastal meteorological station data (herein shortened to coastal stations/data) and then proposes a set of rigorous calibration procedures to compensate for spatial variations in bias. The calibrated data are annually resolved, span 50 years (1958–2007) and represent a much improved accumulation grid in terms of regional and global accuracy. The work also provides regional uncertainties.

## 2. Data

### 2.1. Greenland Ice Sheet Mask

[6] Accurate delineation of an ice sheet mask is important because high coastal accumulation rates have a significant impact on regional and even total ice sheet accumulation rate. Following calibration, the Polar MM5 output is clipped to the extent of the Greenland Ice Sheet using a land surface classification mask. The mask is determined by classification of 1.25 km resolution end-of-summer NASA Moderate Resolution Imaging Spectroradiometer (MODIS) bands 1–4 and 6 cloud-free imagery from 2006. The surface is considered permanent ice, and thus included in the mask, if surface reflectance exceeds 0.3 and if the Normalized Difference Vegetation Index (NDVI) is less than 0.1. The total area of the Greenland Ice Sheet with the mask is $1.75 \times 10^6$ km$^2$, 2.3% larger than the value used by *Ohmura et al.* [1999].

### 2.2. Firn Cores

[7] Accumulation rate data at 215 sites were gathered from four sources: (1) NASA Program for Arctic and Regional Climate Assessment (PARCA) firn cores [*Bales et al.*, 2001a; *McConnell et al.*, 2001; *Mosley-Thompson et al.*, 2001; *Hanna et al.*, 2006], (2) additional recent non-PARCA cores [*Hanna et al.*, 2006], (3) coastal meteorological station data (solid precipitation) [*Ohmura et al.*, 1999; *Cappelen and Kern-Hansen*, 2008], and (4) and pre-PARCA cores tabulated by *Bales et al.* [2001a]. Additional older cores tabulated by *Ohmura and Reeh* [1991] were not used because many were drilled prior to the onset of the Polar MM5 simulation used in this study.

[8] The robustness of our method relies on the accuracy of in situ accumulation rate estimates. Accumulation rate data obtained from firn cores and snow pits are affected by wind-driven snow redistribution and measurement uncertainties [*Mosley-Thompson et al.*, 2001].

[9] Wind redistributes snow, erodes and disturbs stratigraphic layers and creates surface undulations, such as sastrugi, that produce microscale spatial variations in accumulation rate. The result is "glaciological noise" in a firn core time series that may confound the mesoscale accumulation signal. For example, Humboldt Main, North, and East were drilled 25 km apart and have nearly the same mean accumulation rate (148, 144, and 146 mm/yr w.e., respectively) for their period of overlap (1929–1992). But for any single year, accumulation rates vary between the three sites owing to glaciological noise, producing a standard error of 37 mm or 25% of the mean observed accumulation rate. At NASA-U, comparing the main core with 2 other cores 50 m and 2000 m away gives a mean standard error of 41 mm/yr w.e. or 12% of their mean annual accumulation rate [*Anklin et al.*, 1998; *Mosley-Thompson et al.*, 2001].

[10] Different seasonally varying parameters (e.g., $\delta^{18}$O, dust concentration, etc.) may be used to identify annual layers in firn cores. The timing of the minimum and/or maximum value varies among the different seasonal indicators. Isotopic diffusion in firn can smooth the annual $\delta^{18}$O signal in older years, increasing uncertainty, particularly in lower accumulation regions [*Johnsen*, 1977].

[11] PARCA cores were dated using annual variations in dust concentration, $\delta^{18}$O, $H_2O_2$ and $NO_3^-$, along with beta radioactivity horizons from 1963 and 1952 thermonuclear bomb testing [*Anklin et al.*, 1998]. For most of the cores, the individual parameters agree on the number of years within each core, suggesting the dating is reliable. However, the timing of the oscillations varies from year to year and between parameters. Thus, the thickness of a specific annual layer derived from different seasonal indicators may vary substantially, even when the time scales are identical [*Mosley-Thompson et al.*, 2001].

[12] Dating errors and glaciological noise can be minimized with temporal averaging [*Mosley-Thompson et al.*, 2001; *Cogley*, 2004; *Monaghan et al.*, 2006]. The temporal averaging required to attain spatially representative values is longer for low-accumulation regions (i.e., 20 years for Humboldt, ~140 mm/yr w.e.) and shorter for higher-accumulation regions (i.e., 10 years for NASA-U, ~330 mm/yr w.e.) [*Mosley-Thompson et al.*, 2001].

[13] Point measurements of accumulation rate on the ice sheet spatially autocorrelate within a range of 150–200 km [*Bales et al.*, 2001a; *McConnell et al.*, 2001]; in other words, data from any one observation site cannot be expected to be representative of areas more distant than 150–200 km. Correlation-length scales, as such, impose spatial limits when interpolating accumulation directly from sparse in situ measurements. However, our method interpolates Polar MM5 accumulation rate bias, rather than accumulation rate itself. The spatial autocorrelation range of Polar MM5 accumulation rate bias is much larger than that of measured accumulation rate alone; therefore, our method is less vulnerable to sparsely distributed core sites than if the core accumulation rate data were interpolated directly.

## 2.3. Coastal Precipitation Observations

[14] Including coastal data provides estimates of Polar MM5 bias along the coast but when used to infer accumulation rates on the ice sheet, the coastal stations are suspect for biases themselves. The Danish Meteorological Institute (D.M.I.) reports precipitation at 40 sites near sea level along the Greenland coast, most often with a standard Hellmann gauge and Nipher wind shield [*Ohmura et al.*, 1999]. The D.M.I. data do not distinguish between solid and liquid precipitation. *Ohmura et al.* [1999] inferred solid precipitation using an empirical relationship between mean monthly temperature and the fraction of solid precipitation and included a gauge under-catch correction. This study utilized the corrected coastal data used by *Ohmura et al.* [1999]. *Cappelen and Kern-Hansen* [2008] provided a technical report on the original D.M.I. station data.

[15] Three potential sources of bias exist within the coastal data when used for Polar MM5 calibration.

[16] 1. The coastal data provide solid precipitation data, not accumulation rate data, and the relation between solid precipitation on the coast and accumulation rate on the ice sheet is unknown. Our calibration assumes the coastal data to be accumulation rate data, leading to a probable overestimation of accumulation rate along the coasts.

[17] 2. *Ohmura et al.* [1999] introduced an opposing source of bias by using monthly mean, rather than daily wind speeds for under-catch correction, possibly underestimating precipitation by about 15% on average, but as much as 50% for some stations [*Bales et al.*, 2009].

[18] 3. Steep coastal terrain and microclimatic differences between the coastal stations and the inland ice, add complexity not accounted for explicitly in this work. Much of the precipitation over inland ice is orographic and, as such, is underestimated by the meteorological stations near sea level. We partially address the bias associated with orographic effects in section 4.2.

## 3. Model Description

### 3.1. Polar MM5

[19] The Polar MM5 [*Bromwich et al.*, 2001; *Cassano et al.*, 2001; *Box et al.*, 2004, 2006, 2009] is a source of Greenland Ice Sheet accumulation rate estimates. The model contains specialized modifications including explicit ice-phase cloud microphysics, polar physical parameterizations for cloud-radiation interactions, an optimal stable boundary layer turbulence parameterization, improved treatment of heat transfer through snow and ice surfaces, and implementation of a sea ice surface type. The model run used for this study has 24 km horizontal resolution over a 2904 km by 2424 km domain. It is reinitialized every 30 days using 2.5° horizontal resolution analyses from the European Center for Medium-Range Weather Forecasting (ECMWF) 40-year reanalysis (ERA-40, which actually covers more than 40 years) from 1958 to 2002, and ECMWF operational analyses from 2002 to 2005. Boundary conditions are forced using the same data sets, which are sufficient for modeling synoptic motion at the lateral boundaries.

[20] The Polar MM5 has separate outputs for solid and liquid precipitation and surface water vapor transfer ($E$). Blowing snow sublimation ($Q_s$) is calculated off line using the procedure of *Déry and Yau* [2001]. Retained liquid precipitation, $E$ and $Q_s$ are small but significant components of accumulation rate; they comprise < 1%, 11%, and 6% of total accumulation rate, respectively [*Janssens and Huybrechts*, 2000; *Box et al.*, 2004]. All of these terms can be combined to produce a Polar MM5 accumulation rate output. Unfortunately, $E$ values from our Polar MM5 run were not useable for this study owing to processing errors. We found that including retained liquid precipitation, $E$ and $Q_s$ in our unadjusted accumulation rate data set ultimately does not improve our calibrated model accuracy. Therefore, we calibrate Polar MM5 solid precipitation output, not accumulation rate output, implicitly accounting for surface and blowing snow–water vapor fluxes. Indeed, the spatial patterns of E and $Q_s$ are lost, but these terms, especially $Q_s$, are inadequately understood and subsequently are likely to be poorly modeled by the Polar MM5.

[21] Non-Polar MM5 simulations were found to contain systematic precipitation biases on steep windward slopes in the Pacific Northwest of the United States [*Colle et al.*, 1999, 2000]. Finer model resolution improved overall performance, but the non-Polar MM5 underestimated precipitation on steep windward slopes when the topography was poorly resolved and overestimated precipitation when topography was well resolved [*Colle et al.*, 2000]. Overestimation biases at fine resolutions were attributed to shortcomings in the MM5's microphysical parameterization. Such biases are unlikely to affect our accumulation rate estimates because less than 0.5% of the Greenland Ice Sheet area is steeper than 5°, with steep topography confined to a negligible portion of the coastal area.

### 3.2. Resampling of Polar MM5 Output

[22] Because the Polar MM5 grid resolution is too coarse to resolve the tortuous coastline and outlet glaciers, we bilinearly interpolate the Polar MM5 data to 1.25 km. The interpolation scheme does not affect our accumulation rate estimates, but does allow much more precise delineation of the ice sheet boundary than in the NCAR land surface classification data [*Chen and Dudhia*, 2001] used in Polar MM5.

## 4. Data Processing

### 4.1. In Situ Data Selection

[23] The in situ data were screened to assure data quality. Twenty-five sites were omitted for the following reasons: (1) fourteen sites had duplicate entries, (2) four cores were drilled on an ice mass disconnected from the main ice sheet

**Figure 1.** Locations of 105 cores and 28 coastal stations used for the Polar MM5 calibration separated into calibration regions (for clarity, not all are labeled). Omitted cores are also included.

on a peninsula in the Lincoln Sea and had outlying values with respect to inland ice data, (3) five coastal stations lie outside the Polar MM5 grid, and (4) the Crawford Point 1 core obtained in 1995 was disrupted by melt and probably flawed during extraction. The remaining 190 sites were filtered to account for two issues: (1) each site needed to have a record long enough for temporal averaging to minimize glaciological noise [*Mosley-Thompson et al.*, 2001], and (2) 73 sites did not have annual resolution and report only a single long-term mean accumulation rate for a period beginning prior to Polar MM5 runs. While it is impossible to make a contemporaneous comparison between these in situ observations and Polar MM5 output, simply removing these points substantially deteriorates the spatial coverage of available sites. Therefore, we chose to include such in situ data and make the assumption that there have not been significant changes in long-term mean accumulation rate on the Greenland Ice Sheet; any errors associated with using old core
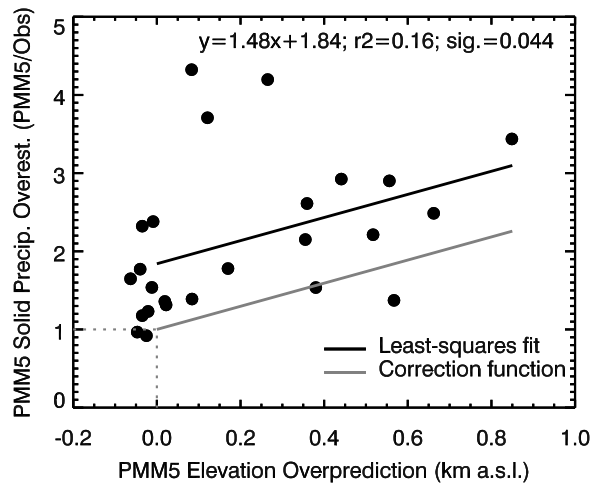
**Figure 2.** Polar MM5 precipitation bias at coastal stations shown as a function of the difference between modeled and actual station elevation. The black line is a linear fit to the data displayed, and the gray line represents the function used to add an elevation-dependent proportion to the coastal data.

data are stochastic and would accordingly average to minimal values. This assumption may not be entirely sound. *Bales et al.* [2001b] found no linear trend in observed accumulation rate in the northwest over the past 250 years; however, they did find interdecadal fluctuations at individual core sites of 25%, although the majority of the annual fluctuations were less than 5%. If, there has been an increase in accumulation rate, our assumption would lead to an underestimation of ice sheet–wide accumulation rates.

[24] To minimize the temporal sampling problems outlined in the previous paragraph, we require each site to coincide with the Polar MM5 model runs (1958–2007) for at least 10 or 20 years for high and low accumulation rate sites, respectively [*Mosley-Thompson et al.*, 2001]. Since wind redistribution is probably less of a problem for coastal data, we required at least seven years of contemporaneous data from each coastal station. Additionally, we removed NGT14-B18 because it reports only a single mean accumulation rate for a particularly long period (897A.D.: 1997), during which accumulation rates may have been lower [*Box et al.*, 2009]. Fifty-seven sites failed to meet these requirements, leaving 133 sites for our calibration. Figure 1 illustrates the spatial distribution of all available sites, including those omitted.

### 4.2. Coastal Precipitation Adjustments

[25] The 28 coastal stations used for our calibration are all located within 77 m of sea level and are typically surrounded by mountainous terrain. Complex terrain is poorly represented by the 24 km Polar MM5 grid resolution averaged from 0.625 km terrain data [*Ekholm*, 1996]. Consequently, the elevation of the Polar MM5 terrain model coincident with the coastal stations averages ~200 m higher than the true elevation of the stations. Orographic precipitation is directly linked to the elevation gradient [e.g., *Ohmura and Reeh*, 1991]; therefore, an inconsistency in elevation between the coastal stations and the Polar MM5

will likely contribute to a positive bias in modeled precipitation. Since we intend to use the coastal data to calibrate the Polar MM5, we adjust the coastal data to represent the precipitation at an elevation equivalent to the Polar MM5 terrain model.

[26] The discrepancy between modeled and observed precipitation at the coastal stations is dependent on the discrepancy between the Polar MM5 terrain and the true elevation of each coastal station; see the black line in Figure 2. The *y*-intercept (ordinate) of the linear fit represents bias unrelated to elevation that may be due to microphysical parameterizations [*Colle et al.*, 2000] and/or systematic underestimation of coastal precipitation despite gauge corrections by *Ohmura et al.* [1999]. The slope of the line suggests that if the Polar MM5 terrain were 500 m higher than a coastal station, we should expect the Polar MM5 bias to be ~1.3 times higher than if the Polar MM5 terrain matched the true elevation of the coastal station. To compensate for this orographic bias, we proportionally increase each station's observed accumulation rate according to the gray line in Figure 2. The correction significantly reduces Polar MM5 versus coastal station noise and bias (Figure 3).

[27] The orographic correction cannot account for errors in the solid/liquid precipitation fraction between the Polar MM5 terrain and the station data. Assuming a dry adiabatic lapse rate of $-9.8°C/km$, the Polar MM5 would average $2.0°C$ colder than the temperature at the coastal station elevations, thus leading to more solid precipitation. Such a discrepancy could lead to an additional elevation-dependent bias. However, reevaluating the correction of the original DMI gauge data is beyond the scope of this study.

[28] After orographic correction, we assume the gauge data are accurate on average (Figure 3). While any remaining disagreement between the Polar MM5 and the coastal stations could be due to elevation/temperature discrepancies, precipitation measurement/correction problems, and Polar MM5 inadequacies, our Polar MM5 calibration assigns all further
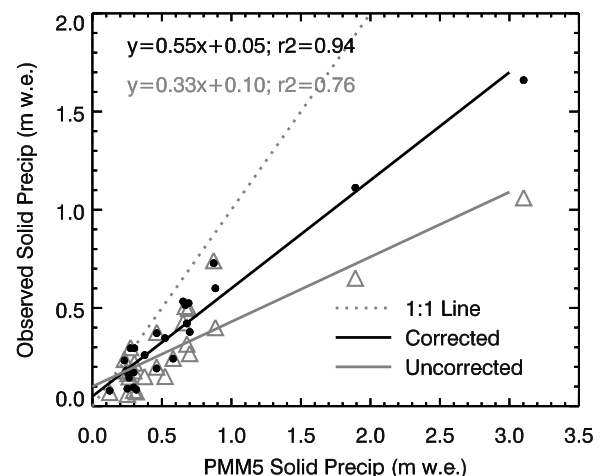


**Figure 3.** The results of correcting the coastal data for the orographic/elevation bias. The two outlying points are Aputiteeq and Tingmiarmiut (locations in Figure 1). Note that the linear fits in the plot are heavily affected by Aputiteeq and Tingmiarmiut and are not used in the calibration. A linear fit to the coastal data excluding Aputiteeq and Tingmiarmiut is shown in Figure 6.
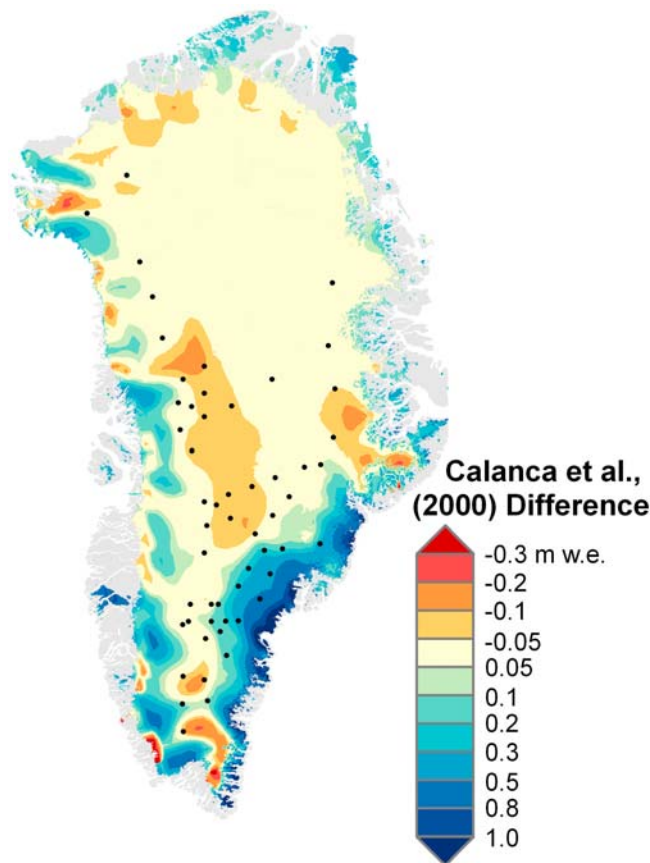
**Figure 4.** Polar MM5 mean accumulation rate from 1958 to 2007 minus accumulation rate map from *Calanca et al.* [2000]. Blue and red indicate that Polar MM5 is higher and lower, respectively. Annually resolved in situ sites used for examining temporal patterns in Polar MM5 bias and for calculating annual uncertainty estimates are overlaid.

disagreement to Polar MM5. Any remaining bias in the coastal data will lead to a bias within our calibration. Despite these probable biases, we expect that the inclusion of coastal data will lead to a better result than excluding them, but without coastal data free of the biases discussed in section 2.3, we cannot evaluate this assumption.

## 5. Polar MM5 Calibration

### 5.1. Polar MM5 Bias

[29] A calibration scheme that compensates for all regional and/or temporal variations in bias will be more accurate than a "global" calibration like that applied by *Box et al.* [2006]. Temporal and spatial patterns in bias were examined independently. Temporal patterns in bias were examined by calculating the mean annual difference between measured accumulation rate at all available annually resolved in situ sites (Figure 4) and Polar MM5 solid precipitation. Results showed no significant temporal variations in the Polar MM5 biases, including periods post and prior to 1979, when additional satellite-derived vertical water vapor and temperature profiling data became available to the global analyses driving the regional Polar MM5 simulations. Additionally, Polar

MM5 solid precipitation bias does not correlate with the North Atlantic Oscillation (NAO) index (J. Hurrell, NAO Index Data Provided by the Climate Analysis Section, 1958 to 2003, National Center for Atmospheric Research, Boulder, Colorado, 1995, available at http://www.cgd.ucar.edu/cas/jhurrell/indices.html), while the Polar MM5 precipitation rate does [*Box*, 2005].

[30] Spatial patterns in bias, however, do emerge and are illustrated in Figure 5. We define bias empirically as the ratio between the mean observed accumulation rate for all available years at each site and the contemporaneous mean Polar MM5 solid precipitation. Throughout the interior above ~2000 m, Polar MM5 solid precipitation is consistently 25% higher than in situ data. Biases are less consistent on the coasts and ice margin but remain spatially coherent. Along the western ice sheet margin, Polar MM5 bias is slightly more positive (overestimation) than in the interior. The southeastern ice sheet is the only area where Polar MM5 consistently underestimates accumulation rate. The coastal stations suggest stronger Polar MM5 overestimations than seen with the firn cores, which is indicative of orographic and/or under-catch correction biases within the coastal data. Aputiteeq and Tingmiarmiut (coastal stations), have extreme outlying positive biases, consistent with our hypothesis regarding their failure to capture orographic intensification of precipitation.

[31] Examining Polar MM5 bias in a bias space, as shown in Figure 6, reveals that these spatial patterns, generally, conform to one of three linear functions. The majority of the core data fits tightly to the dark line and is very well constrained. Cores in the southeast, however, do not follow the same pattern; instead they fit less tightly, to a nearly parallel line situated higher in the bias space. The coastal stations have more noise, as would be expected, but fit to a line slightly flatter than that for the interior.

[32] Four sites (GITS, Basin 4 (at the southern tip), Aputiteeq, and Tingmiarmiut; Figure 1) show incongruous biases that are likely real and not erroneous. GITS is in an area of pronounced orographic precipitation, upslope from the mesoscale low-pressure system in northern Baffin Bay [*Ohmura and Reeh*, 1991; *Box et al.*, 2004]. Basin 4 is at the southern tip of the ice sheet in a region with strong horizontal gradients owing to orography [*Box et al.*, 2004] and should receive precipitation from both westerly and southerly storm tracks. The southeast coastal stations have extremely high precipitation rates due to orographic intensification associated with close proximity to the vigorous Icelandic Low/North Atlantic storm track [see *Serreze et al.*, 1993]. Mapping the residuals of the data shown in Figure 6 shows no coherent spatial patterns, which suggests that these three linear functions (excepting four abnormal sites) account for all of the spatial variation in bias that is possible to extract from this noisy data.

### 5.2. Calibration Procedure

[33] Persistent surface undulations on the ice sheet and small-scale topographic changes on the coasts contribute a considerable amount of noise to the bias data discussed above. When using the bias data to develop a calibration surface for the Polar MM5, it is important to exclude that noise, as including it would insert additional error into the calibrated data set. Conventional methods, such as
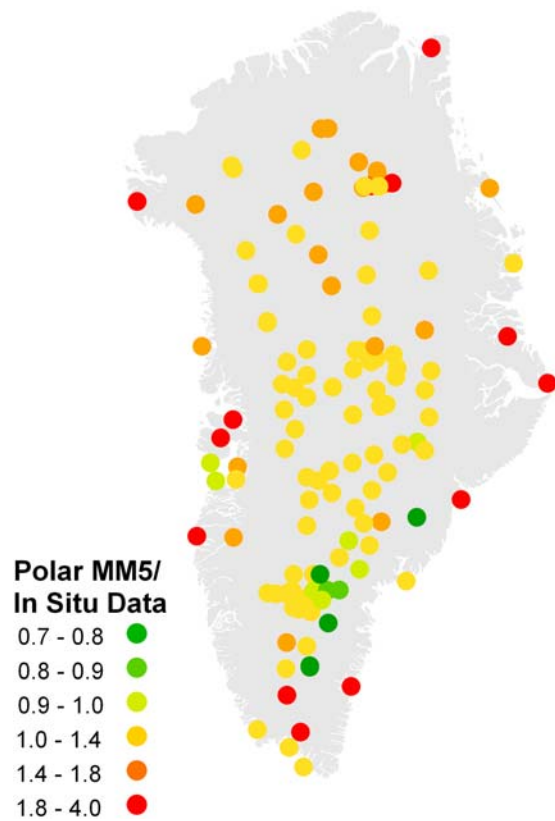
**Figure 5.** Average Polar MM5 bias at all sites using each site's or model's contemporaneous time period. Red and green indicate Polar MM5 overestimation and underestimation, respectively.

straightforward spatial interpolation or spatial regression, cannot filter out noise and are consequently ineffective when dealing with noisy data sets. Our calibration uses an unconventional method designed to build a calibration surface for the Polar MM5 that filters out noise in the bias data while still capturing all coherent spatial variations in bias.

[34] As stated in section 5.1, all coherent spatial variation in Polar MM5 bias can be explained with three linear functions, each representing a specific region on the ice sheet. Distinguishing which in situ sites belong to each region could not be done empirically owing to noise within the bias data, thus was done manually. Discriminating each site's logical region was unambiguous except four the four unique sites discussed in section 5.1. These sites were treated separately, as discussed in the following. The three major regions are the interior ice sheet, the southeast coast, and coastal stations.

[35] A linear best fit correction function was derived for the three main regions, with the mean Polar MM5 solid precipitation set as the independent variable and the mean observed accumulation rate set as the dependent variable (Table 1). A spatial weighting scheme insured that areas with denser sampling were not favored in the regressions. Site density was calculated using a Gaussian function with a sigma value equivalent to 1/2 the spatial autocorrelation range of accumulation rate (calculated by fitting a spherical model to a semivariogram of our annually resolved core data). A correction function with a $y$-intercept of 0 implies that all bias is proportional to the accumulation rate; this logical trait is

contained in the interior and coastal station correction functions. From an empirical standpoint, a $y$-intercept greater than zero implies a constant underestimation of accumulation rate that is independent of the accumulation rate itself. This may not be intuitive but is seen in the southeast (Table 1); there, the $y$-intercept of 237 mm/yr w.e. may be a consequence of the limited number of sites within the region. Despite the illogical $y$-intercept for the southeast correction function, we chose to use the function because it is optimal for minimizing bias. Forcing the southeast correction function through zero increases our final accumulation rate estimate by only 1.3%.

[36] The aforementioned sites that showed incongruous biases contained insufficient data to perform a linear fit; instead, we defined a linear correction function that passes through the origin, and the single point within the bias space representing the GITS, Basin 4 and the mean of the three coastal stations (Tasiilaq was included owing to its proximity to Aputiteeq, and Tingmiarmiut). This method assumes all bias is proportional to accumulation rate.

### 5.3. Spatial Interpolation

[37] Spatial interpolation of the coefficients and constants of the regional linear correction functions creates a gridded, spatially varying correction function. Several interpolation methods were considered: kriging, cokriging with elevation, local polynomial fits, inverse distance weighting (IDW), normalized difference weighting (NDW), and triangulated irregular networks (TINs). A TIN performed best, producing uniform values within the regions and realistic transitions between regions (for lattice, see Figure 7). Other methods were suboptimal; kriging requires a Gaussian distribution of $Z$-values that the data could not satisfy. Other methods failed to generate constant $Z$-values within each region.
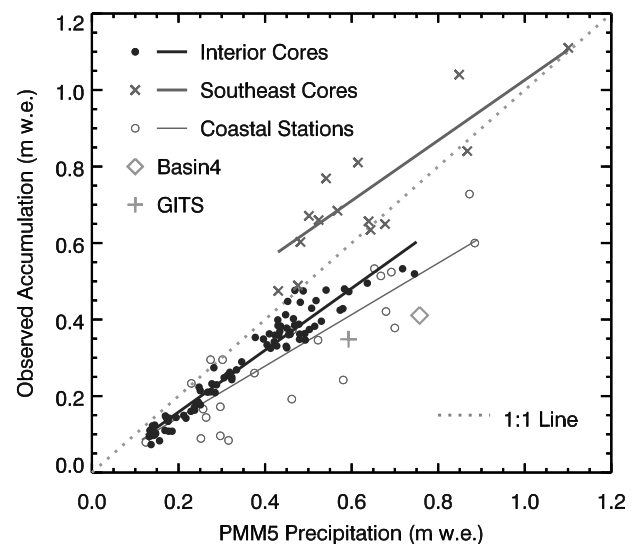


**Figure 6.** Bias patterns divided into regional groups: interior, southeast, and coastal stations with spatially weighted regional correction functions overlaid. GITS and Basin 4 are also shown. The mean value of Tasiilaq, Aputiteeq, and Tingmiarmiut is off the scale of this plot. The point would lie at 1.95 and 1.18 for Polar MM5 and observed, respectively.

**Table 1.** Regional Correction Functions Derived From Comparison Between Polar MM5 and in Situ Data[a]

| Region | Constant | Coefficient |
|---|---|---|
| Central ice sheet | −4 | 0.801 |
| Southeast ice sheet | 237 | 0.789 |
| Coastal stations | −9 | 0.673 |
| Southeast coastal stations | 0 | 0.604 |
| GITS | 0 | 0.588 |
| Basin 4 | 0 | 0.543 |

[a]Constants represent units of mm/yr w.e.

[38] Areas outside the TIN boundary were extrapolated by assigning the value of the closest interpolated cell. This extrapolation constitutes a negligible source of error. The final TINs were passed through a Gaussian low-pass spatial filter to remove sharp boundaries. The transitions between regions are largely controlled by the relative locations of the core sites and coastal stations; thus, we advise caution when using this data set to infer accumulation rate in areas transitioning between regions. The coefficient and constant surfaces were used to spatially calibrate all years of Polar MM5 solid precipitation output. The impact of the calibration on the original data set is illustrated in Figure 7. Since the Polar MM5 solid precipitation was primarily calibrated to in situ accumulation rate data, we herein consider the calibrated Polar MM5 data set to represent accumulation rate.

## 6. Uncertainty Estimation

[39] Uncertainty is calculated as the root-mean-square error (RMSE) between the calibrated Polar MM5 and in situ accumulation rate data for both the annually resolved accumulation rate estimates and the 50 year mean accumulation rate estimate (1958–2007). Uncertainty estimates use the same in situ data as used for the calibration because there is insufficient in situ data to make independent calibration and uncertainty data sets. Hence, we are careful to limit the circularity of our uncertainty estimates. Our calibration removes systematic biases detected at 133 sites each averaged over at least 10 years and did not remove bias on a site-by-site or year-by-year basis. For example, at the site of a firn core, the calibrated Polar MM5 is not calibrated to that single core, rather the calibration adjusts the accumulation rate equally for all years according to a systematic pattern contained within all of the cores in the region. Therefore, the nonsystematic error remains unaltered in calibrated Polar MM5 accumulation rate grid data and it is the nonsystematic error that we are defining as uncertainty. GITS and Basin 4 are exceptions because their correction functions were fit directly through a single point (section 5.2), thus the temporally averaged RMSE equaled zero. Methods used to remove circular uncertainty estimates for GITS and Basin 4 are addressed in sections 6.1 and 6.2. Uncertainty estimates for the annually resolved accumulation rates are still valid for all sites, including GITS and Basin 4, because the annual variations in uncertainty remain unaltered in the calibrated Polar MM5 accumulation rate data.

### 6.1. Annual Uncertainty

[40] Estimating annual accumulation rate uncertainty requires annually resolved in situ data. Of the 133 sites available for calibration of the Polar MM5, only the 58 PARCA cores have annually resolved values (Figure 4). Observed annual accumulation rate at these sites was compared to the calibrated Polar MM5 accumulation and was found to be noisy but generally proportional to the accumulation rate. Given the amount of noise within the uncertainties, we chose to estimate uncertainty at all grid points in the Polar MM5 using the same method as done with the calibration. The spatial distribution of uncertainty is different than that of bias and reflects the spatial pattern of accumulation rate. We divided the cores into three regions accordingly: the southeast (identical to the region used for the bias correction), the northern ice sheet (accumulation rates generally less than 350 mm/yr w.e.) and the southern ice sheet (accumulation rates generally greater than 350 mm/yr w.e.), separated at 70.5° N latitude. The uncertainty at GITS, Basin 4 and the southeast coastal stations was consistent with other nearby sites, thus they were placed into their respective large-scale regions.
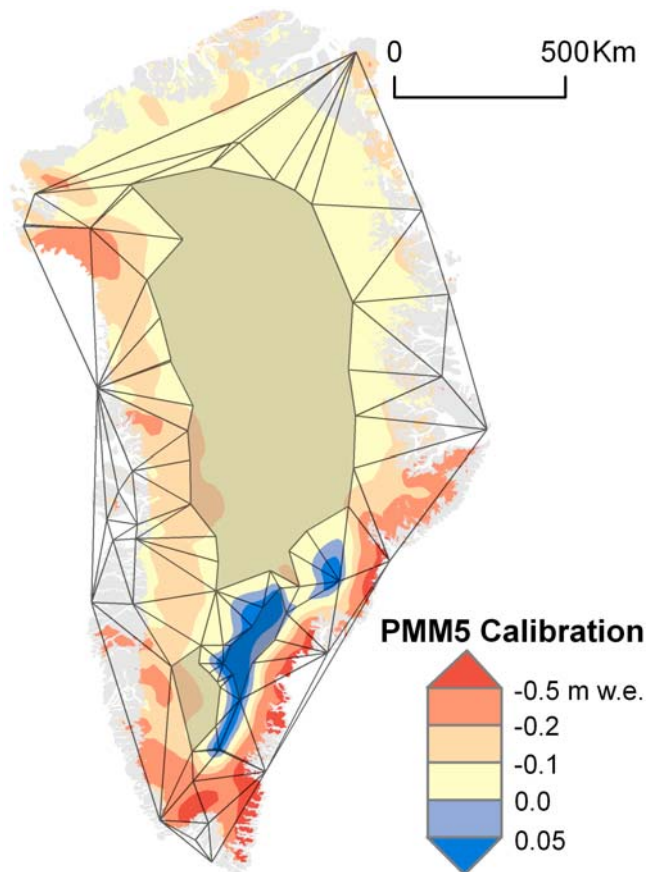


**Figure 7.** Corrected Polar MM5 accumulation rate minus the uncorrected Polar MM5 solid precipitation rate. Triangulated irregular network (TIN) lattice used to spatially interpolate the regional coefficients and constants across the Polar MM5 domain is overlaid. Gray polygons represent areas where the correction function is constant over space.
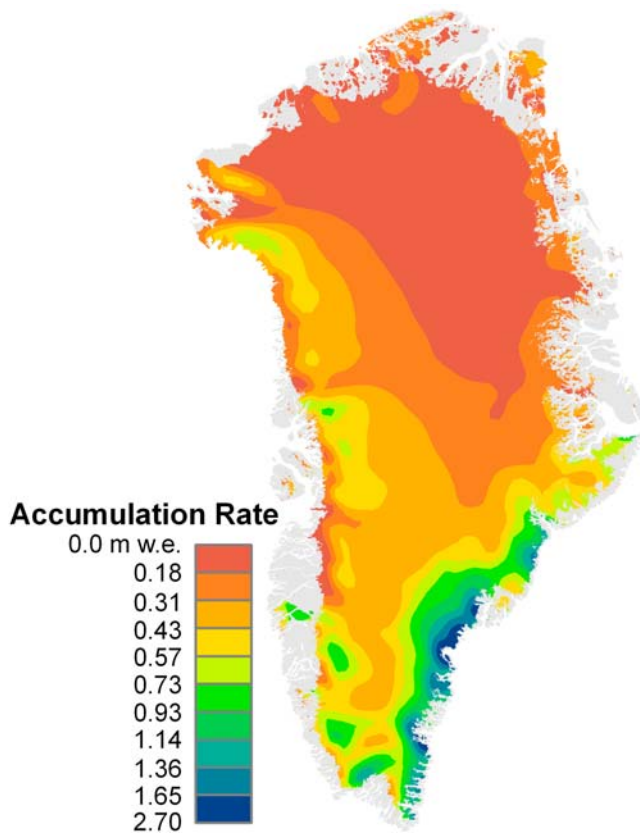
**Figure 8.** Calibrated Polar MM5 average accumulation rate map for the period 1958–2007.

[41] A RMSE is calculated for each core separately, and the mean RMSEs for each region are spatially interpolated with a TIN. The PARCA cores have no sites in the northeast or within 100 km of the ice margin; thus we extrapolate our uncertainty estimates into these areas. No smoothing is applied to the uncertainty TIN. The mean ice sheet–wide uncertainty is defined as the mean of the uncertainty surface within the ice sheet mask. GITS and Basin 4 actually increase the overall annual uncertainty. These uncertainty estimates attribute all disagreement between the calibrated Polar MM5 and the in situ data to the Polar MM5. In reality, the uncertainties in annual firn core estimates are considerable and will contribute to some unknown portion of the error.

### 6.2. Temporally Averaged Uncertainty

[42] Estimating temporally averaged uncertainty did not require annually resolved observations; therefore all 133 sites were used to obtain the most robust result possible. Again, uncertainty exhibited a noisy but regional pattern generally reflecting the spatial pattern of accumulation rate. Regional delineations for temporally averaged uncertainty were very similar to those chosen for the annual uncertainty but had to be slightly different since 133 points were available instead of 58. We identified four regions of similar uncertainty: the coastal stations, the southeast, the remaining portion of the ice sheet with accumulation rates higher than 350 mm/yr w.e. (southern ice sheet and west coast) and areas with accumulation rates less than 350 mm/yr w.e. (north interior and northeast ice sheet). Again, GITS, Basin 4

and the southeast coastal stations were grouped with their respective larger regions. At each site, the mean observed accumulation rate was compared to mean calibrated Polar MM5 accumulation rate at the appropriate grid point for the contemporaneous years. RMSE values were calculated for each region and then spatially interpolated as was done for the annually resolved values. Including GITS, Basin 4 and the southeast coastal stations in the uncertainty estimates increased the mean ice sheet RMSE by 0.73 mm/yr w.e. Mean ice sheet–wide RMSE was calculated as the mean value of the uncertainty surface within the ice sheet mask.

## 7. Results

### 7.1. Greenland Net Accumulation Rate

[43] A temporally averaged 1958–2007 accumulation rate map is displayed in Figure 8. Within the ice sheet mask of $1.74 \times 10^6$ km, the total average accumulation rate (1958–2007) is 339 mm/yr w.e. or 591 Gt/yr, a value 21% or 103 Gt/yr higher than given by the *Calanca et al.* [2000] grids and ∼22% higher than that of *Cogley* [2004]. Note that the whole ice sheet values are not directly comparable owing to differing ice sheet masks used, but overall, *Calanca et al.* [2000] and *Cogley* [2004] grids are very similar, differing by only a few Gt/yr. We find that whole ice sheet values are very sensitive to how the land/ice/sea mask is defined, especially along the southeast ice margin where accumulation rates are extremely high (Figures 4 and 8). Calibrated Polar MM5 accumulation rates are also higher than most previously published regional climate model results: 75 Gt/yr higher than that of *Box et al.* [2006] and 104 Gt/yr higher than that of *Hanna et al.* [2006]. *Ettema et al.* [2009] find a higher accumulation rate of 697 Gt/yr (J. Bamber, personal communication, 2009) that may be a result of finer spatial resolution. But most importantly, *Ettema et al.* [2009] show very similar patterns of high accumulation rates along the southeast coast. Calibrated Polar MM5 accumulation rates for the southern interior, the north and the west agree well with the *Cogley* [2004] and *Calanca et al.* [2000] mean grid (herein referred to as CAL/COG), averaging 5 mm/yr w.e. higher. Excluding the southeast, Polar MM5 1958–2007 interior ice sheet (above 2000 m) accumulation rates are insignificantly lower (−0.9 mm/yr w.e.) than CAL/COG and 71 mm/yr w.e. (42 Gt/yr) higher along the coasts. Localized areas along the west margin show larger disagreement with CAL/COG up to ±200 mm/yr w.e.

[44] In the southeast, the calibrated Polar MM5 mean accumulation rates exceed CAL/COG by 135 mm/yr w.e. (23 Gt/yr) above 2000 m and by 601 mm/yr w.e. (48 Gt/yr) below 2000 m (Figure 4). Our maximum mean accumulation rate is 2150 mm w.e., 770 mm/yr w.e. greater than that of *Calanca et al.* [2000] and 950 mm/yr w.e. greater than that of *Cogley* [2004]. Southeast firn cores agree more closely with our larger estimate than with that of *Calanca et al.* [2000] or of *Cogley* [2004]. The calibrated Polar MM5 indicates that although the southeast ice sheet comprises only 14% of the ice sheet area, it receives 31% of Greenland's mass accumulation. Gravity measurements indicate the southeast dominates Greenland's mass balance variability and is currently losing more mass than anywhere else on the ice sheet [e.g., *Luthcke et al.*, 2006; *Wouters et al.*,

2008]. Our results suggest that the same region also dominates ice sheet–wide accumulation and that a significant proportion of the southeast's mass balance variability is likely due to accumulation rate variability.

[45] It is also noteworthy that the uncorrected Polar MM5 solid precipitation was higher than CAL/COG in the southeast, while the southeast cores indicated that the uncorrected Polar MM5 was still underpredicting accumulation. Thus, in higher-elevation areas along the southeast slope, the calibration increased both the accumulation rate and the disagreement between the Polar MM5 and CAL/COG. Extremely high accumulation rates in the southeast have actually been accepted for sometime [e.g., *Bromwich et al.*, 1998] but have been omitted by most accumulation analyses. Recent improvements to coastal data gauge correction by *Bales et al.* [2009] have produced kriged accumulation rate maps that show southeast accumulation rates higher and closer to the calibrated Polar MM5 than CAL/COG or *Bales et al.* [2001a].

[46] The only in situ data collected in the low-elevation portion of the southeast ice sheet are from the Dome Greenpeace core, a 15.5 m firn core drilled at 62°10.80′ N, 42°24.38′ W (714 m a.s.l.) in July 2005. Here, Polar MM5 simulated a peak mean accumulation rate of 2780 mm/yr w.e., and established accumulation rate data sets derived from spatial interpolation [*Calanca et al.*, 2000] predicted 880 mm/yr w.e. Annual layer thickness was established using isotopic and dust analyses; accumulation rates for hydrologic years 2003–2004 and 2004–2005 were 4240 mm/yr w.e. and 3280 mm/yr w.e., respectively (J. E. Box, unpublished data, 2005). Although there was melt and rain in this area, the nature of the layers suggests that little mass was able to percolate through to older years, thus little mass was lost. Noteworthy is that these coastal accumulation rates are much larger than the values simulated by calibrated Polar MM5 of 2620 and 2670 mm/yr w.e., respectively. This is not unexpected given the extreme precipitation gradients in the area. However, given the known biases within the coastal data (section 2.3), particularly in the context of under-catch, the Dome Greenpeace core supports the possibility that accumulation rates in the southeast may be even higher than estimated by the calibrated Polar MM5.

## 7.2. Temporal Accumulation Variability

[47] The calibrated Polar MM5 results indicate that the mean interannual variability over the entire ice sheet has a standard deviation of 62 mm/yr w.e., 109 Gt/yr, or 18%. The temporal variability of the calibrated Polar MM5 is slightly less than that of the core data; this is to be expected given that the core data includes additional sources of noise discussed in section 2.2. Polar MM5 also indicates that accumulation rate variability is generally higher on the relatively low elevation ice sheet periphery (Figure 9). The southeast ice sheet exhibits high interannual variability (Figure 9) that is nearly an order of magnitude larger than in much of the interior, with an 18% or 33 Gt/yr standard deviation. Thus, the southeast not only receives 31% of Greenland's accumulated mass, it also accounts for 30% of Greenland's total interannual variability in accumulated mass. Furthermore, the southeast ice sheet below 2000 m encompasses only 5% of the Greenland Ice Sheet's total

area, yet accounts for 17% of its total interannual variability in accumulation rate.

[48] A linear regression of Polar MM5 ice sheet–wide annual accumulation rate shows a significant, though minor, increase in accumulation of 7 mm/yr w.e. decade$^{-1}$ ($R^2$ = 0.11, $F$ test: sig. = 0.018). This increase is better described by a step function, increasing approximately 32 mm/yr w.e. or 10% (sig. $p < 0.01$) between 1968 and 1972 (Figure 10). The stepwise increase appears to be the result of a combination of events. First, prior to 1962, the calibrated Polar MM5 shows anomalously low accumulation rates in the west and anomalously high accumulation rates in the east (Figure 11). Around 1965 this pattern reverses, with an anomalous accumulation rate minimum in the east and high anomalies in the west. This pattern continues until a steep transition between 1968 and 1972 (Figure 10). Caution must be taken when considering this transition, as 1972 was when the ERA-40 began assimilation of the first primitive satellite sounder information—the NOAA Vertical Temperature Profile Radiometer (VTPR)—that could impact detection of cyclonic activity in the ice-free North Atlantic. However, the 1972 precipitation increase is readily observable in both the southeast firn core data (Figure 10) and in eastern coastal stations [*Bales et al.*, 2009].

[49] *Josey and Marsh* [2005] detected an identical temporal precipitation pattern from independent rain gauge measurements in Iceland and NCEP/ERA-40 reanalyses, which has contributed to a freshening of the North Atlantic subpolar gyre. They attribute this event primarily to an abrupt change in the wintertime East Atlantic Pattern that was far more negative in the late 1960s than it has been since. The majority of the core data do not include this pattern but this is not surprising. The Polar MM5 indicates that change occurred largely on low-elevation southeastern slopes of the ice sheet where there are only four cores with sufficiently long, annually resolved records; those four cores clearly indicate the 1968–1972 accumulation rate increase (Figure 10).

[50] The anomalously low accumulation rates on the west coast during the late 1950s and early 1960s is not discernable in the observational record; however, an accumulation rate increase may still exist because the majority of the in situ data begin in the early 1960s. The western increase broadly coincides with the accumulation rate decrease on the east slope as well as a pronounced negative minimum in the winter NAO and winter East Atlantic Pattern (EAP) in 1964 (J. Hurrell, NAO Index Data Provided by the Climate Analysis Section, 1958 to 2003, National Center for Atmospheric Research, Boulder, Colorado, 1995, available at http://www.cgd.ucar.edu/cas/jhurrell/indices.html). This is a reasonable explanation as storm tracks might approach up the west coast rather than passing along the southeast coast, which is expected with a negative NAO [see *Rogers et al.*, 2004]. However, this explanation does not explain why the southwest accumulation rate does not decrease around 1972 while NAO and EAP increase.

[51] No significant change in ice sheet–wide accumulation rate is evident after 1972 (Figure 10) including recent years (~1998 to present) when surface air temperatures have increased [e.g., *Box et al.*, 2006]. There is an apparent, though insignificant, accumulation rate increase primarily on the western ice sheet after 1992 (Figure 11), while accumulation
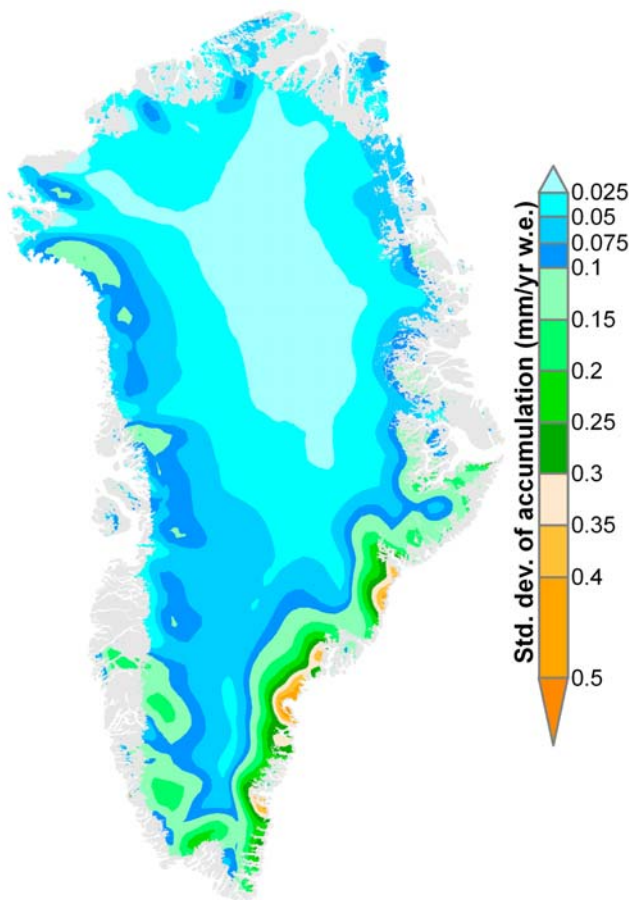
and regional temporal correlation coefficients are displayed in Table 2. We consider these numbers to be a lower bound on our actual uncertainties for two reasons.

[54] 1. Our assumption that all in situ data are unbiased may not be valid for the coastal data. After orographic correction, the Polar MM5 coastal station bias was still fractionally higher than the firn core bias. Our application of coastal precipitation data as accumulation rate data would have the opposite impact. Thus, a fractionally larger positive bias indicates that either the Polar MM5 is systematically fractionally overestimating precipitation in all coastal areas, more so than anywhere else, or the use of monthly mean wind speeds to correct coastal data for gauge under-catch probably underestimates accelerated winds during storm events and thus, probably underestimated precipitation rate. If the former is the culprit, our calibration corrected these biases. If it is the latter, our accumulation rate data set still underestimates accumulation rates along the coasts. Recent use of daily wind speeds has already yielded higher precipitation rates [*Bales et al.*, 2009].

[55] 2. The annual accumulation rate RMSE was derived without data from coastal regions where annual uncertainty is unknown and where orographic effects can be important. Although our annual uncertainties were derived with little data from the northern ice sheet, we expect our estimates there to be relatively accurate. Temporally averaged accu-
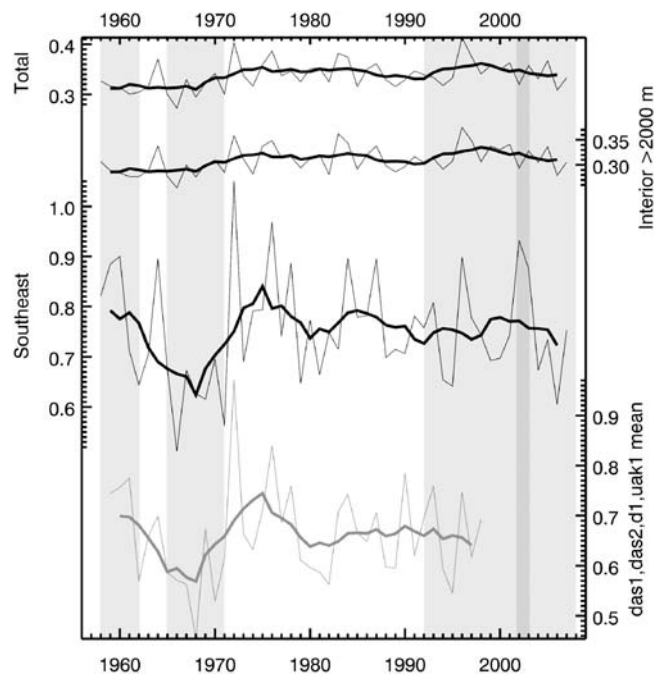


**Figure 9.** Standard deviation of accumulation rate (1958–2007) from calibrated Polar MM5. Color scale is not linear.

rates in the southeast decreased slightly. The extreme high-accumulation seasons of 2002–2003 observed by both in situ data at NASA-SE [*Nghiem et al.*, 2005] and by altimetry studies indicating recent high-elevation interior thickening [*Thomas et al.*, 2006; *Krabill et al.*, 2004; *Johannessen et al.*, 2005] appear to be mostly confined to the southeast (Figure 10), as also shown by *Hanna et al.* [2006].

[52] Throughout the 1958–2007 study period three spatial patterns prevail (Figure 11). First, accumulation rate anomalies are strongest on the ice sheet periphery and weakest in the high-elevation interior. Second, accumulation rates on the east and west sides of the ice sheet are anticorrelated. The anticorrelation is not significant, though the pattern is unequivocal during certain time periods, as shown in Figure 11. Third, the high-accumulation rate variability along the southeast coast has a great influence on total ice sheet–wide accumulation rates.

### 7.3. Calibrated Polar MM5 Uncertainty

[53] The mean ice sheet–wide RMSE as described in sections 6.1 and 6.2 is 75 mm/yr w.e., 22% or 131 Gt/yr for annual accumulation rate and 48 mm/yr w.e., 14% or 83 Gt/yr for temporally averaged accumulation rate. Annual RMSE shows no significant temporal trends, nor significant correlations with the NAO and EAP. Regional RMSEs



**Figure 10.** Time series of calibrated Polar MM5 mean accumulation rates for the entire ice sheet, the interior ice sheet, and the southeast (black). The mean accumulation rate at four southeast cores (das1, das2, d1 and uak1) is shown in gray. The *y* axes represent accumulation rate in m w.e. and are scaled equally for all time series. Thicker lines represent a 7 year Gaussian smoothing. All southeast cores with full-length records are included in the southeast core time series. The lightly shaded areas represent the time periods shown in Figure 11. The dark shaded area represents the 2002–2003 "high accumulation" years.
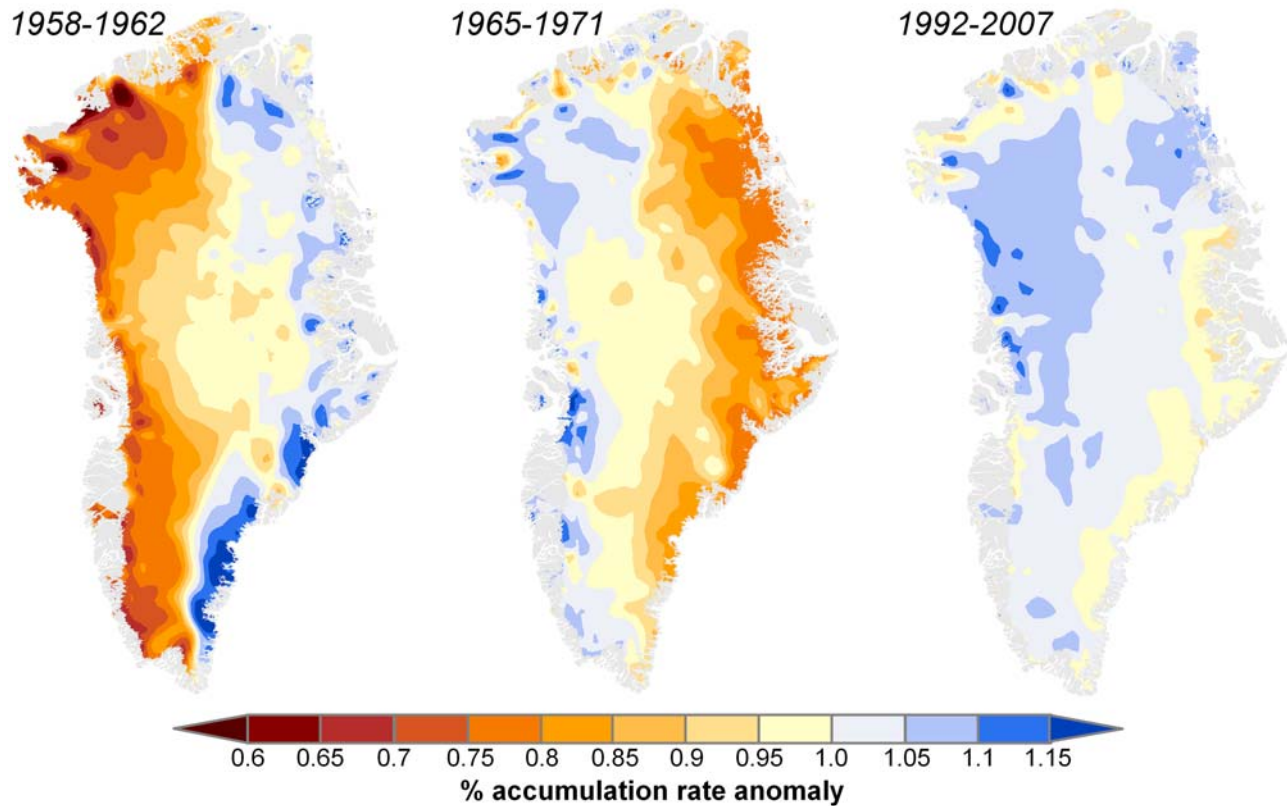
**Figure 11.** Percent accumulation rate anomaly maps for three distinct periods. Periods are also displayed as gray shading in Figure 10.

mulation rate uncertainties in northeast Greenland lack mesoscale structure, suggesting that processes affecting accumulation rate are consistent throughout northeast Greenland. While uncertainties in the northeast can be up to 60% of the total accumulation rate, the total volume uncertainty is only 35% of the total ice sheet uncertainty because accumulation rates there are so small. Estimated annual RMSE likely overestimates uncertainties for the interior because glaciological noise within the firn core data is included in the annual RMSE estimates.

## 8. Conclusions

[56] Independent firn cores and meteorological station records are used to identify and correct spatially varying systematic biases in Polar MM5 regional climate model solid precipitation output. The result: an annually resolved data set of Greenland Ice Sheet accumulation rate with improved accuracy, absolute uncertainty estimates and minimal biases when compared to our in situ data (Figure 1). The data set, with accompanying metadata, is available for download at http:/bprc.osu.edu/Greenland_accumulation/.

[57] We are able to sidestep the complexities of surface and blowing snow–water vapor fluxes by compensating for the difference between Polar MM5 solid precipitation and accumulation rate, including Polar MM5 errors implicitly. We do not, however, gauge the loss factor due to surface and blowing snow–water vapor fluxes, which has spatial and temporal variability resulting from independent factors such as downslope accelerating katabatic winds and inter-

annual variability in temperature and lower tropospheric moisture content. Thus, an improved accounting of regional climate model error may partition surface and blowing snow–water vapor fluxes from total precipitation to more directly assess intrinsic model biases.

[58] We have established that the use of coastal data to estimate Greenland Ice Sheet accumulation rates must include an orographic correction. In addition, the use of monthly mean wind speeds to correct coastal data for gauge under-catch likely underestimates accelerated winds during storm events thus probably underestimates precipitation rate.

[59] We estimate that the 1958–2007 Greenland Ice Sheet average snow accumulation rate is $337 \pm 48$ mm/yr w.e. or $591 \pm 83$ Gt/yr, a value ~21% higher than that of *Calanca et al.* [2000] based on that of *Ohmura et al.* [1999] and ~16% higher than that of *Cogley* [2004]. We attribute our higher reported value to better representation of high orographic precipitation along the ice sheet margins, particularly in the southeast, where accumulation rates are 71 Gt/yr higher than previously thought, accounting for one third of Greenland's total accumulation.

[60] Additionally, interannual accumulation rate variability in the southeast is large enough to significantly impact the total mass budget of the entire ice sheet, accounting for approximately one third of the ice sheet's total interannual variability in accumulation. Between 1958 and 2007, the only significant variation in Greenland's annual accumulation rate, confirmed with in situ observations, is due to an accumulation rate minimum that occurred almost exclusively in the southeast from 1965 to 1971, coincident with a strong

**Table 2.** Calibrated Polar MM5 Uncertainties Derived From Comparison Between Calibrated Polar MM5 and in Situ Data[a]

| Annual Uncertainty | RMSE | Mean Correlation |
|---|---|---|
| Southern ice sheet | 89 | 0.567 |
| Southeast | 165 | 0.415 |
| Northern ice sheet | 58 | 0.487 |
| Ice sheet–wide | 75 | 0.501 |

| Temporally Averaged Uncertainty | RMSE | Percent RMSE |
|---|---|---|
| Interior high accumulation | 38 | 9.7 |
| Interior low accumulation | 18 | 10.7 |
| Southeast | 86 | 12.1 |
| Coastal stations | 92 | 23.5 |
| Ice sheet–wide | 48 | 14.2 |

[a]RMSEs represent units of mm/yr w.e. Annual correlation coefficients are calculated temporally at each site and then averaged throughout each region. Percent RMSE is the RMSE divided by the mean modeled accumulation rate.

negative East Atlantic Pattern. We emphasize that accumulation rates on the Greenland Ice Sheet vary regionally but not uniformly.

[61] These findings have important implications for resolving the total mass budget in southeast Greenland, both in the context of ice sheet modeling and in monitoring changes in mass on an annual basis. A 71 Gt/yr increase in mean accumulation rate and higher accumulation rate variability in the southeast is enough to change the sign of Greenland mass balance in some years.

[62] The fact that previous Greenland accumulation studies have underestimated the importance of the southeast emphasizes that the paucity of data in this region is problematic and is consequently limiting our understanding of a region critical to estimating Greenland accumulation. Therefore, collecting in situ data in the low-elevation southeast ice sheet and minimizing uncertainties within in situ data are vital steps toward resolving Greenland accumulation uncertainties.

## References

Anklin, M., R. C. Bales, E. Mosley-Thompson, and K. Steffen (1998), Annual accumulation at two sites in northwest Greenland during recent centuries, *J. Geophys. Res.*, 103(D22), 28,775–28,783, doi:10.1029/98JD02718.

Bales, R. C., J. R. McConnell, E. Mosley-Thompson, and B. Csatho (2001a), Accumulation over the Greenland Ice Sheet from historical and recent records, *J. Geophys. Res.*, 106(D24), 33,813–33,825, doi:10.1029/2001JD900153.

Bales, R. C., E. Mosley-Thompson, and J. R. McConnell (2001b), Variability of accumulation in northwest Greenland over the past 250 years, *Geophys. Res. Lett.*, 28(14), 2679–2682, doi:10.1029/2000GL011634.

Bales, R. C., Q. Guo, D. Shen, J. R. McConnell, G. Du, J. F. Burkhart, V. B. Spikes, E. Hanna, and J. Cappelen (2009), Annual accumulation for Greenland updated using ice core data developed during 2000–2006 and analysis of daily coastal meteorological data, *J. Geophys. Res.*, 114, D06116, doi:10.1029/2008JD011208.

Benson, C. S. (1962), Stratigraphic studies in the snow and firn of the Greenland Ice Sheet, *Res. Rep. A245733*, U.S. Snow, Ice, and Permafrost Res. Estab., Wilmette, Ill.

Box, J. E. (2005), Greenland Ice Sheet surface mass-balance variability: 1991–2003, *Ann. Glaciol.*, 42, 90–94, doi:10.3189/172756405781812772.

Box, J. E., and A. Rinke (2003), Evaluation of Greenland Ice Sheet surface climate in the HIRHAM regional climate model using automatic weather station data, *J. Clim.*, 16(9), 1302–1319.

Box, J. E., D. H. Bromwich, and L.-S. Bai (2004), Greenland Ice Sheet surface mass balance 1991–2000: Application of Polar MM5 mesoscale model and in situ data, *J. Geophys. Res.*, 109, D16105, doi:10.1029/2003JD004451.

Box, J. E., L. Yang, J. Rogers, D. Bromwich, L.-S. Bai, K. Steffen, J. Stroeve, and S.-H. Wang (2005), Extreme precipitation events over Greenland: Consequences to ice sheet mass balance, paper 5.2 presented at 8th International Conference on Polar Meteorology and Oceanography, *Am. Meteorol. Soc.*, San Diego, Calif., 9–13 Jan.

Box, J. E., D. H. Bromwich, B. A. Veenhuis, L.-S. Bai, J. C. Stroeve, J. C. Rogers, K. Steffen, T. Haran, and S.-H. Wang (2006), Greenland Ice Sheet surface mass balance variability (1988–2004) from calibrated Polar MM5 output, *J. Clim.*, 19(12), 2783–2800, doi:10.1175/JCLI3738.1.

Box, J. E., L. Yang, D. H. Bromwich, and L.-S. Bai (2009), Greenland Ice Sheet surface air temperature variability: 1840–2007, *J. Clim.*, 22(14), 4029–4049, doi:10.1175/2009jcli2816.1.

Bromwich, D. H., R. I. Cullather, Q. Chen, and B. M. Csathó (1998), Evaluation of recent precipitation studies for Greenland Ice Sheet, *J. Geophys. Res.*, 103(D20), 26,007–26,024, doi:10.1029/98JD000044.

Bromwich, D. H., J. J. Cassano, T. Klein, G. Heinemann, K. M. Hines, K. Steffen, and J. E. Box (2001), Mesoscale modeling of katabatic winds over Greenland with the Polar MM5, *Mon. Weather Rev.*, 129, 2290–2309, doi:10.1175/1520-0493(2001)129<2290:MMOKWO>2.0.CO;2.

Calanca, P., H. Gilgen, S. Ekholm, and A. Ohmura (2000), Gridded temperature and accumulation distributions for Greenland for use in cryospheric models, *Ann. Glaciol.*, 31, 118–120, doi:10.3189/172756400781820345.

Cappelen, J., and C. Kern-Hansen (2008), Guide to climate data and information from the Danish Meteorological Institute, *Tech. Rep. 08-10*, Dan. Meteorol. Inst., Copenhagen.

Cassano, J. J., J. E. Box, D. H. Bromwich, L. Li, and K. Steffen (2001), Evaluation of Polar MM5 simulations of Greenland's atmospheric circulation, *J. Geophys. Res.*, 106(D24), 33,867–33,889, doi:10.1029/2001JD900044.

Chen, F., and J. Dudhia (2001), Coupling an advanced land surface-hydrology model with the Penn State-NCAR MM5 modeling system. Part I: Model implementation and sensitivity, *Mon. Weather Rev.*, 129, 569–585, doi:10.1175/1520-0493(2001)129<0569:CAALSH>2.0.CO;2.

Cogley, J. G. (2004), Greenland accumulation: An error model, *J. Geophys. Res.*, 109, D18101, doi:10.1029/2003JD004449.

Colle, B. A., K. J. Westrick, and C. F. Mass (1999), Evaluation of MM5 and Eta-10 precipitation forecasts over the Pacific Northwest during the cool season, *Weather Forecasting*, 14(2), 137–154, doi:10.1175/1520-0434(1999)014<0137:EOMAEP>2.0.CO;2.

Colle, B. A., C. F. Mass, and K. J. Westrick (2000), MM5 precipitation verification over the Pacific Northwest during the 1997–99 cool seasons, *Weather Forecasting*, 15(6), 730–744, doi:10.1175/1520-0434(2000)015<0730:MPVOTP>2.0.CO;2.

Déry, S., and M. Yau (2001), Simulation of blowing snow in the Canadian arctic using a double-moment model, *Boundary Layer Meteorol.*, 99(2), 297–316, doi:10.1023/A:1018965008049.

Dethloff, K., et al. (2002), Recent Greenland accumulation estimated from regional climate model simulations and ice core analysis, *J. Clim.*, 15(19), 2821–2832, doi:10.1175/1520-0442(2002)015<2821:RGAEFR>2.0.CO;2.

Ekholm, S. (1996), A full coverage, high-resolution, topographic model of Greenland computed from a variety of digital elevation data, *J. Geophys. Res.*, 101(B10), 21,961–21,972, doi:10.1029/96JB01912.

Ettema, J., M. R. van den Broeke, E. van Meijgaard, W. J. van de Berg, J. L. Bamber, J. E. Box, and R. C. Bales (2009), Higher surface mass balance of the Greenland Ice Sheet revealed by high-resolution climate modeling, *Geophys. Res. Lett.*, 36, L12501, doi:10.1029/2009GL038110.

Fettweis, X., E. Hanna, H. Gallée, P. Huybrechts, and M. Erpicum (2008), Estimation of the Greenland Ice Sheet surface mass balance for the 20th and 21st centuries, *Cryosphere*, 2, 117–129.

Glover, R. W. (1999), Influence of spatial resolution and treatment of orography on GCM estimates of the surface mass balance of the Greenland Ice Sheet, *J. Clim.*, *12*(2), 551–563, doi:10.1175/1520-0442(1999) 012<0551:IOSRAT>2.0.CO;2.

Hanna, E., P. Huybrechts, I. Janssens, J. Cappelen, K. Steffen, and A. Stephens (2005), Runoff and mass balance of the Greenland Ice Sheet: 1958–2003, *J. Geophys. Res.*, *110*, D13108, doi:10.1029/2004JD005641.

Hanna, E., A. Stephens, J. McConnell, S. Das, and J. Cappelen (2006), Observed and modeled Greenland Ice Sheet snow accumulation, 1958–2003, and links with regional climate forcing, *J. Clim.*, *19*(3), 344–358, doi:10.1175/JCLI3615.1.

Hanna, E., P. Huybrechts, K. Steffen, J. Cappelen, R. Huff, C. Shuman, R. Irvine-Fynn, S. Wise, and M. Griffiths (2008), Increased runoff from melt from the Greenland Ice Sheet: A response to global warming, *J. Clim.*, *21*(2), 331–341, doi:10.1175/2007JCLI1964.1.

Janssens, I., and P. Huybrechts (2000), The treatment of meltwater retention in mass-balance parameterization of the Greenland Ice Sheet, *Ann. Glaciol.*, *31*, 133–140, doi:10.3189/172756400781819941.

Johannessen, O. M., K. Khvorostovsky, M. W. Miles, and L. P. Bobylev (2005), Recent ice-sheet growth in the interior of Greenland, *Science*, *310*(5750), 1013–1016, doi:10.1126/science.1115356.

Johnsen, S. J. (1977), Stable isotope homogenization of polar firn and ice, *IAHS AISH Publ.*, *118*, 210–219.

Josey, S. A., and R. Marsh (2005), Surface freshwater flux variability and recent freshening of the North Atlantic in the eastern subpolar gyre, *J. Geophys. Res.*, *110*, C05008, doi:10.1029/2004JC002521.

Krabill, W., et al. (2004), Greenland Ice Sheet: Increased coastal thinning, *Geophys. Res. Lett.*, *31*, L24402, doi:10.1029/2004GL021533.

Luthcke, S. B., H. J. Zwally, W. Abdalati, D. D. Rowlands, R. D. Ray, R. S. Nerem, F. G. Lemoine, J. J. McCarthy, and D. S. Chinn (2006), Recent Greenland ice mass loss by drainage system from satellite gravity observations, *Science*, *314*(5803), 1286–1289, doi:10.1126/science. 1130776.

McConnell, J. R., R. C. Bales, D. Belle-Oudry, J. D. Kyne, G. Lamorey, E. Hanna, and E. Mosley-Thompson (2001), Annual net snow accumulation over southern Greenland from 1975 to 1998, *J. Geophys. Res.*, *106*(D24), 33,827–33,837, doi:10.1029/2001JD900129.

Monaghan, A. J., et al. (2006), Insignificant change in Antarctic snowfall since the International Geophysical Year, *Science*, *313*(5788), 827–831, doi:10.1126/science.1128243.

Mosley-Thompson, E., J. R. McConnell, R. C. Bales, Z. Li, P.-N. Lin, K. Steffen, L. G. Thompson, R. Edwards, and D. Bathke (2001), Local to regional-scale variability of annual net accumulation on the Greenland Ice Sheet from PARCA cores, *J. Geophys. Res.*, *106*(D24), 33,839–33,851, doi:10.1029/2001JD900067.

Murphy, B. F., I. Marsiat, and P. Valdes (2002), Atmospheric contributions to the surface mass balance of Greenland in the HadAM3 atmospheric model, *J. Geophys. Res.*, *107*(D21), 4556, doi:10.1029/2001JD000389.

Nghiem, S. V., K. Steffen, R. Huff, and G. Neumann (2005), Anomalous snow accumulation over the southeast region of the Greenland Ice Sheet during 2002–2003 snow season, paper presented at 8th Conference on Polar Meteorology and Oceanography, Am. Meteorol. Soc., San Diego, Calif.

Ohmura, A., and N. Reeh (1991), New precipitation and accumulation maps of Greenland, *J. Glaciol.*, *37*, 140–148.

Ohmura, A., M. Wild, and L. Bengtsson (1996), A possible change in mass balance of Greenland and Antarctica in the coming century, *J. Clim.*, *9*(9), 2124–2135, doi:10.1175/1520-0442(1996)009<2124:APCIMB>2.0. CO;2.

Ohmura, A., P. Calanca, M. Wild, and M. Anklin (1999), Precipitation, accumulation and mass balance of the Greenland Ice Sheet, *Z. Gletscherkd. Glazialgeol.*, *35*, 1–20.

Rogers, J. C., S.-H. Wang, and D. H. Bromwich (2004), On the role of the NAO in the recent northeastern Atlantic Arctic warming, *Geophys. Res. Lett.*, *31*, L02201, doi:10.1029/2003GL018728.

Serreze, M. C., J. E. Box, and R. G. Barry (1993), Characteristics of Arctic synoptic activity, *Meteorol. Atmos. Phys.*, *51*, 147–164, doi:10.1007/ BF01030491.

Thomas, R., E. Frederick, W. Krabill, S. Manizade, and C. Martin (2006), Progressive increase in ice loss from Greenland, *Geophys. Res. Lett.*, *33*, L10503, doi:10.1029/2006GL026075.

Thompson, S. L., and D. Pollard (1997), Greenland and Antarctic mass balances for present and doubled atmospheric CO2 from the GENESIS version-2 global climate model, *J. Clim.*, *10*(5), 871–900, doi:10.1175/ 1520-0442(1997)010<0871:GAAMBF>2.0.CO;2.

van der Veen, C. J., D. H. Bromwich, B. M. Csatho, and C. Kim (2001), Trend surface analysis of Greenland accumulation, *J. Geophys. Res.*, *106*(D24), 33,909–33,918, doi:10.1029/2001JD900156.

Wouters, B., D. Chambers, and E. J. O. Schrama (2008), GRACE observes small-scale mass loss in Greenland, *Geophys. Res. Lett.*, *35*, L20501, doi:10.1029/2008GL034816.

R. C. Bales, Sierra Nevada Research Institute, University of California, Merced, CA 95343, USA.

J. E. Box, D. H. Bromwich, and E. Mosley-Thompson, Department of Geography, Ohio State University, Columbus, OH 43210, USA.

E. W. Burgess and R. R. Forster, Department of Geography, University of Utah, 260 S. Central Campus Dr., Salt Lake City, UT 84112-9155, USA. (evan.burgess@geog.utah.edu)

L. C. Smith, Department of Geography, University of California, Los Angeles, CA 90024, USA.